JOC Article
pubs.acs.org/joc

Electron-Transfer Properties of Short-Lived *N*-Oxyl Radicals. Kinetic Study of the Reactions of Benzotriazole-*N*-oxyl Radicals with Ferrocenes. Comparison with the Phthalimide-*N*-oxyl Radical

Enrico Baciocchi,[‡] Massimo Bietti,[§] Massimo Di Fusco,[†] Osvaldo Lanzalunga,*[,†,‡] and Daniele Raponi[†]

[†]*Dipartimento di Chimica, Sapienza Università di Roma, piazzale A. Moro, 5 I-00185 Rome, Italy,* [‡]*Istituto CNR di Metodologie Chimiche (IMC-CNR), Sezione Meccanismi di Reazione, c/o Dipartimento di Chimica, Sapienza Università di Roma, piazzale A. Moro, 5 I-00185 Rome, Italy, and* [§]*Dipartimento di Scienze e Tecnologie Chimiche, Università "Tor Vergata", Via della Ricerca Scientifica, I-00133 Rome, Italy*

osvaldo.lanzalunga@uniroma1.it

Received May 7, 2009

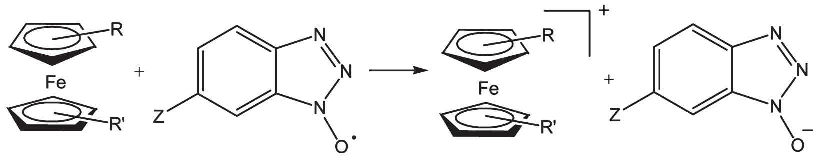

A kinetic study of the one-electron oxidation of a series of substituted ferrocenes (FcX: X = H, $COCH_3$, CO_2Et, CH_2OH, Et, and Me_2) by the benzotriazole-*N*-oxyl radical (BTNO) and of ferrocene (FcH) by a series of ring-substituted benzotriazole-*N*-oxyl radicals (Z-BTNO: Z = H, 6-CF_3, 6-Cl, 6-Me, 6-MeO) has been carried out in CH_3CN. *N*-Oxyl radicals were produced by hydrogen abstraction from 1-hydroxybenzotriazoles (Z-HBT) by the cumyloxyl radical produced after 355 nm laser flash photolysis of a solution of dicumyl peroxide in CH_3CN. In both systems, the rate constants exhibited a satisfactory fit with the Marcus equation allowing us to determine self-exchange reorganization energy values for the BTNO/$BTNO^-$ couple, which resulted in good agreement: 34.7 kcal mol^{-1} from the oxidation of ferrocenes by BTNO and 30.5 kcal mol^{-1} from the oxidation of ferrocene by aryl-substituted Z-BTNO. From the average value of 32.6 kcal mol^{-1} it is possible to calculate a self-exchange rate for the BTNO/$BTNO^-$ couple of 7.6×10^5 M^{-1} s^{-1}, which is 3 orders of magnitude higher than that determined for the PINO/$PINO^-$ couple. The difference in the intrinsic barrier between the two oxidants is so large that it overcomes the thermodynamic factor and the oxidation of ferrocene by BTNO results significantly faster than that by PINO in spite of the higher reduction potential of the latter *N*-oxyl radical. The higher reactivity of BTNO with respect to PINO in an electron-transfer process contrasts with what is observed in hydrogen atom transfer processes where PINO is always more reactive than BTNO due to the higher NO−H bond dissociation energy in *N*-hydroxyphthalimide (HPI) than in HBT (88 vs. 85 kcal mol^{-1}, respectively). Thus, the relative reactivity of PINO and BTNO radicals might represent a criterium to help in the distinction of ET and HAT reactions promoted by these transient *N*-oxyl radicals.

Introduction

Short-lived *N*-oxyl radicals like phthalimide-*N*-oxyl radical (PINO) and benzotriazole-*N*-oxyl radical (BTNO) (Figure 1) are an important class of reactive intermediates which have attracted a great interest in view of the fact that they play an important role in the oxidative degradation of lignin promoted by the laccase/O_2 system mediated by

---

(1) Call, H. P.; Mücke, I. *J. Biotechnol.* **1997**, *53*, 163–202. Li, K.; Xu, F.; Eriksson, K.-E. L. *Appl. Environ. Microbiol.* **1999**, *65*, 2654–2660. Sealey, B. J.; Ragauskas, A. J.; Elder, T. J. *Holzforschung* **1999**, *53*, 498–502. Srebotnik, E.; Hammel, K. E. *J. Biotechnol.* **2000**, *81*, 179–188. Balakshin, M.; Chen, C.-L.; Gratzl, J. S.; Kirkman, A. G.; Jakob, H. *J. Mol. Catal. B: Enzym.* **2001**, *16*, 205–215. Potthast, A.; Rosenau, T.; Fischer, K. *Holzforschung* **2001**, *55*, 47–56. Fabbrini, M.; Galli, C.; Gentili, P. *J. Mol. Catal. B: Enzym.* **2002**, *16*, 231–240. Geng, X.; Li, K.; Xu, F. *Appl. Microbiol. Biotechnol.* **2004**, *64*, 493–496. Annunziatini, C.; Baiocco, P.; Gerini, M. F.; Lanzalunga, O.; Sjögren, B. *J. Mol. Catal. B: Enzym.* **2005**, *32*, 89–96.

(2) Xu, F.; Kulys, J. J.; Duke, K.; Li, K.; Krikstopaitis, K.; Deussen, H.-J. W.; Abbate, E.; Galinyte, V.; Schneider, P *Appl. Environ. Microbiol.* **2000**, *66*, 2052–2056.

(3) Xu, F.; Deuss, H.-J. W.; Lopez, B.; Lam, L.; Li, K. *Eur. J. Biochem.* **2001**, *268*, 4169–4176.

(4) D'Acunzo, F.; Baiocco, P.; Fabbrini, M.; Galli, C.; Gentili, P. *New J. Chem.* **2002**, *26*, 1791–1794.

(5) Baiocco, P.; Barreca, A. M.; Fabbrini, M.; Galli, C.; Gentili, P. *Org. Biomol. Chem.* **2003**, *1*, 191–197.

(6) Cantarella, G.; Galli, C.; Gentili, P. *New J. Chem.* **2004**, *28*, 366–372.

DOI: 10.1021/jo900951c

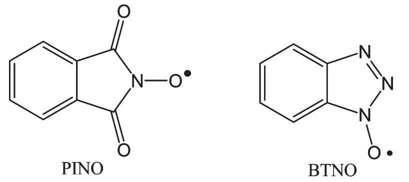

FIGURE 1. Structures of phthalimide-*N*-oxyl radical (PINO) and benzotriazole-*N*-oxyl radical (BTNO).

N-hydroxy derivatives,[1−8] a process that has a potential application in the pulp and paper industry.[9] Moreover PINO is the active oxidant in the synthetically useful metal-catalyzed aerobic oxidation of a wide variety of organic substrates.[10,11]

This interest has stimulated several studies aimed at assessing the mechanism of the reactions of these radicals with a wide variety of organic compounds.[12−22] A hydrogen atom transfer (HAT) mechanism has been generally considered to take place in the reactions of PINO and BTNO radicals with several C−H[16−21] and phenolic O−H bonds.[21,22] Accordingly, in these reactions PINO always displays a higher reactivity than BTNO, which is in line with the larger BDE (88 vs. 85 kcal mol^{-1}) of the O−H bond in *N*-hydroxyphthalimide (HPI) than in *N*-hydroxybenzotriazole (HBT).[8,19,20]

Recently, however, we have shown that in addition to the HAT mechanism also an electron-transfer (ET) mechanism can play a role in the reactions promoted by the PINO radical as in the *N*-demethylation reaction of *N*,*N*-dimethylanilines.[23] This observation led us to investigate the intrinsic ET properties of PINO through a careful study of the ET reaction of PINO with ferrocene and its derivatives.[24] In this study, it was found that the intrinsic barrier for the PINO/PINO$^-$ self-exchange reaction ($\lambda_{\mathrm{PINO/PINO^-}}$) is 49.1 kcal mol^{-1}.

Since the redox potential of the BTNO/BTNO$^-$ couple is quite close to that of the PINO/PINO$^-$ couple[25] a similar reactivity in one-electron oxidations might be foreseen for the two *N*-oxyl radicals. However, practically no information is presently available on the intrinsic tendency of BTNO to undergo ET reactions. Thus, we have felt it of interest to acquire information in this respect, also with the aim of learning about how the structure can influence the intrinsic ET reactivity of short-lived *N*-oxyl radicals. The same approach previously used with PINO has been used and in this paper we now report on a laser photolysis study of the one-electron oxidation of a series of substituted ferrocenes FcX (FcX: X = H, $COCH_3$, CO_2Et, CH_2OH, Et, and Me_2, eq 1) by BTNO in MeCN. In addition, for the sake of completeness, we have also investigated the counterpart system, that is the oxidation of ferrocene by a number of ring-substituted benzotriazole-*N*-oxyl radicals (Z-BTNO, Z = H, 6-CF_3, 6-Cl, 6-Me, and 6-MeO, eq 2).

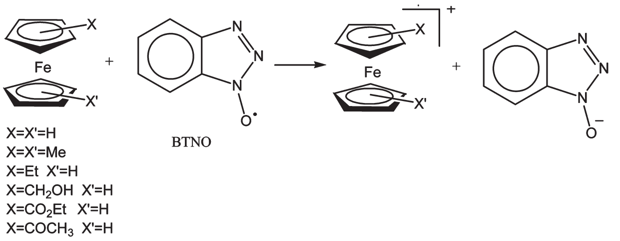

(1)

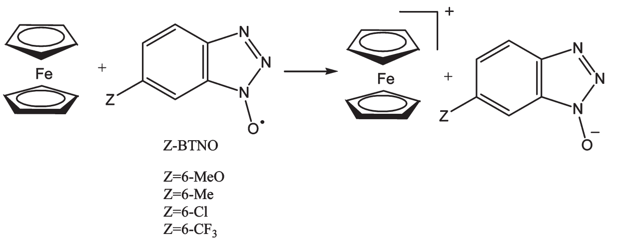

(2)

Results

The analysis of the ET properties of the Z-BTNO radicals required first an investigation of the electrochemical behavior of ring-substituted Z-HBT. The $E°$ values for the Z-BTNO/Z-BTNO$^-$ couples were determined by cyclic voltammetry under the same experimental conditions used for the analysis of the redox potential of the PINO/PINO$^-$ couples.[14,24] Thus, the measurements were carried out with an MeCN solution of Z-HBT (2.0 mM) and Bu_4NBF_4 (0.1 M) as supporting electrolyte in MeCN in the presence of collidine (4 mM), which serves to deprotonate the hydroxylamine moiety giving

---

(7) Branchi, B.; Galli, C.; Gentili, P. *Org. Biomol. Chem.* **2005**, *3*, 2604–2614.

(8) Astolfi, P.; Brandi, P.; Galli, C.; Gentili, P.; Gerini, M. F.; Greci, L.; Lanzalunga, O. *New J. Chem.* **2005**, *29*, 1308–1317.

(9) Argyropoulos, D. S.; Menachem, S. B. *Biotechnology in the Pulp and Paper Industry*; Eriksson, K. E. L., Ed.; Springer-Verlag: Berlin, Germany, 1997; pp 127−158.

(10) Ishii, Y.; Sakaguchi, S.; Iwahama, T. *Adv. Synth. Catal.* **2001**, *343*, 393–427. Minisci, F.; Recupero, F.; Pedulli, G. F.; Lucarini, M. *J. Mol. Catal. A: Chem.* **2003**, *204−205*, 63–90. Minisci, F.; Recupero, F.; Cecchetto, A.; Gambarotti, C.; Punta, C.; Paganelli, R. *Org. Process Res. Dev.* **2004**, *8*, 163–168. Sheldon, R. A.; Arends, I. W. C. E. *Adv. Synth. Catal.* **2004**, *346*, 1051–1071. Yang, G.; Ma, Y.; Xu, J. *J. Am. Chem. Soc.* **2004**, *126*, 10542–10543. Ishii, Y.; Sakaguchi, S. *Catal. Today* **2006**, *117*, 105–113. Chen, Y.-X.; Qian, L.-F.; Zhang, W.; Han, B. *Angew. Chem., Int. Ed.* **2008**, *47*, 9330–9333.

(11) Recupero, F.; Punta, C. *Chem. Rev.* **2007**, *107*, 3800–3842.

(12) Hermans, H.; Vereecken, L.; Jacobs, P. A.; Peeters, J. *Chem. Commun.* **2004**, 1140–1141. Bozzelli, J. W.; da Silva, G. *J. Phys. Chem. C* **2002**, *111*, 5760–5765.

(13) Ueda, C.; Noyama, M.; Ohmori, H.; Masui, M. *Chem. Pharm. Bull.* **1987**, *35*, 1372–1377.

(14) Gorgy, K.; Lepretre, J.-C.; Saint-Aman, E.; Einhorn, C.; Einhorn, J.; Marcadal, C.; Pierre, J.-L. *Electrochim. Acta* **1998**, *44*, 385–393.

(15) Kishioka, S.; Yamada, A. *J. Electroanal. Chem.* **2005**, *578*, 71–77. Kishioka, S.; Yamada, A. *Electrochim. Acta* **2006**, *51*, 4582–4588.

(16) Wentzel, B. B.; Donners, M. P. J.; Alsters, P. L.; Feiters, M. C.; Nolte, R. J. M. *Tetrahedron* **2000**, *56*, 7797–7803. Minisci, F.; Punta, C.; Recupero, F.; Fontana, F.; Pedulli, G. F. *J. Org. Chem.* **2002**, *67*, 2671–2676. Koshino, N.; Cai, Y.; Espenson, J. H. *J. Phys. Chem. A* **2003**, *107*, 4262–4267. Koshino, N.; Saha, B.; Espenson, J. H. *J. Org. Chem.* **2003**, *68*, 9364–9370. Cai, Y.; Koshino, N.; Saha, B.; Espenson, J. H. *J. Org. Chem.* **2005**, *70*, 238–243. Coniglio, A.; Galli, C.; Gentili, P.; Vadalà, R. *Org. Biomol. Chem.* **2009**, *7*, 155–160.

(17) Minisci, F.; Recupero, F.; Cecchetto, A.; Gambarotti, C.; Punta, C.; Faletti, R.; Paganelli, R.; Pedulli, G. F. *Eur. J. Org. Chem.* **2004**, 109–119.

(18) Annunziatini, C.; Gerini, M. F.; Lanzalunga, O.; Lucarini, M. *J. Org. Chem.* **2004**, *69*, 3431–3438.

(19) Galli, C.; Gentili, P.; Lanzalunga, O. *Angew. Chem., Int. Ed.* **2008**, *47*, 4790–4796.

(20) Brandi, P.; Galli, C.; Gentili, P. *J. Org. Chem.* **2005**, *70*, 9521–9528.

(21) Amorati, R.; Lucarini, M.; Mugnaini, V.; Pedulli, G. F.; Minisci, F.; Recupero, R.; Fontana, F.; Astolfi, P.; Greci, L. *J. Org. Chem.* **2003**, *68*, 1747–1754.

(22) Baciocchi, E.; Gerini, M. F.; Lanzalunga, O. *J. Org. Chem.* **2004**, *69*, 8863–8866.

(23) Baciocchi, E.; Bietti, M.; Gerini, M. F.; Lanzalunga, O. *J. Org. Chem.* **2005**, *70*, 5144–5149.

(24) Baciocchi, E.; Bietti, M.; Di Fusco, M.; Lanzalunga, O. *J. Org. Chem.* **2007**, *72*, 8748–8754.

(25) In MeCN, using pyridine as the deprotonating base, the $E°$ value for BTNO (0.97 V vs. NHE)[8,20] is not much different from that reported for the PINO radical (0.78 V vs. SCE).[13]

TABLE 1. Redox Potentials ($E°$) of the Z-BTNO/Z-BTNO$^-$ Couples in CH_3CN at 25 °C[a] and Visible Absorption Maxima of Z-BTNO Radicals

N-oxyl radical	$E°$ (V vs. SCE)[b]	λ_{max} (nm)
6-CF_3-BTNO	0.76	450
6-Cl-BTNO	0.70	465
BTNO	0.63[c]	475
6-Me-BTNO	0.60	480
6-MeO-BTNO	0.58	485
PINO	0.69[d]	380[d]

[a] Z-HBT (2.0 mM) and Bu_4NBF_4 (0.1 M) as supporting electrolyte in the presence of collidine (4 mM). Sweep scan 500 mV/s. [b] Errors < ±0.01 V. [c] Reference 26. [d] Reference 24.

the Z-BTNO$^-$ anion. An Ag/AgCl (KCl, 3 M) electrode was used as reference and the sweep scan was 500 mV/s. The CVs (see Figure S1 in the Supporting Information) exhibit an anodic peak at E_{pa} corresponding to the one-electron oxidation of the Z-BTNO$^-$ to the corresponding *N*-oxyl radical Z-BTNO. The reduction of the electrogenerated radical occurs at E_{pc}. The $E°$ values, equal to $(E_{pa}+E_{pc})/2$ and referred to SCE, are reported in the second column of Table 1.

The $E°$ values clearly indicate that the oxidizing character of the electrogenerated Z-BTNO radicals is significantly dependent on the ring substituents, regularly increasing by increasing the electron-withdrawing power of the Z-substituent. A difference of 180 mV is observed between the more oxidizing 6-CF_3-BTNO and the less oxidizing 6-MeO-BTNO radicals. A good linear correlation ($r^2 = 0.993$) is obtained by plotting the $E°$ values against the σ_p constants of the Z substituents as shown in Figure 2.

The electronic effect of the aryl substituent on the redox potential may be rationalized on the basis of the negative charge delocalization in the aryl ring of Z-BTNO$^-$, in particular in the 6-position as shown in the resonance form **B** displayed in Figure 3. Interestingly, a quite smaller substituent effect on the $E°$ values was observed in the series of the aryl-substituted PINO/PINO$^-$ couples,[27] where a difference of only 60 mV was observed for the redox potentials of the 4-CO_2Me-PINO/4-CO_2Me-PINO$^-$and 4-MeO-PINO/4-MeO-PINO$^-$ couples.[14] We will come back on this point later on.

The occurrence of the oxidation reactions described in eqs 1 and 2 was first demonstrated spectrophotometrically by generating the Z-BTNO radicals by reaction of Z-HBT with $Pb(OAc)_4$ in CH_3CN.[28,29] In all cases it was observed that when a solution of FcX is mixed with a solution of Z-BTNO, the absorption of the *N*-oxyl radical in the visible region is immediately replaced by that of the ferrocenium ion (600−750 nm).[30] As an example, Figure 4 shows the UV−vis spectra of a solution containing $Pb(OAc)_4$ (0.1 mM) and HBT (3 mM) in CH_3CN in the absence (solid line) or in the presence (dashed line) of ferrocene (1 mM). (The UV−vis spectra for the addition of substituted ferrocenes to BTNO and of ferrocene to Z-BTNO radicals are reported in Figures S2−S9 in the Supporting Information).

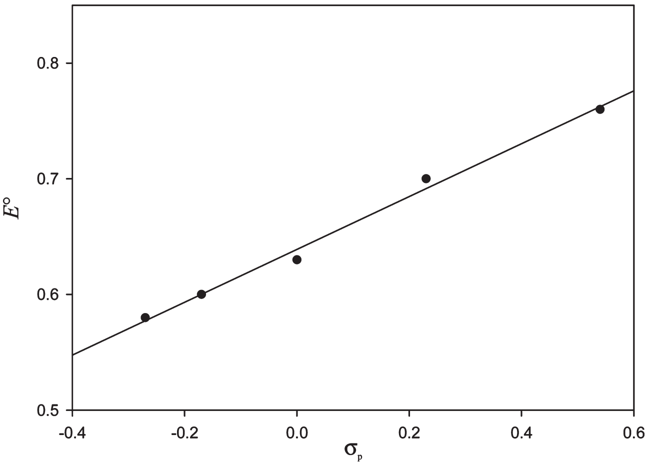

FIGURE 2. Correlation between the $E°$ values for the Z-BTNO/Z-BTNO$^-$ couples and the Hammett σ_p constants of the Z substituents.

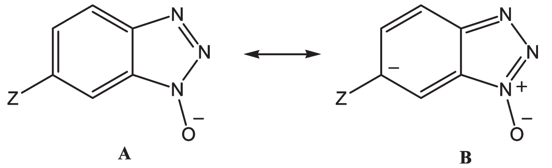

FIGURE 3. Two resonance structures for Z-BTNO$^-$.

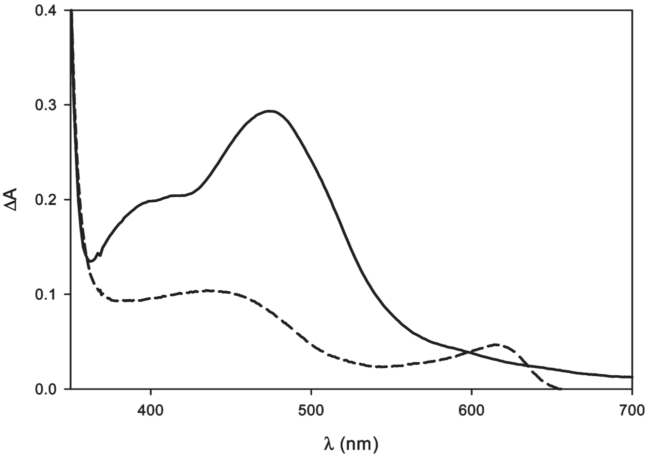

FIGURE 4. UV−vis spectra of a CH_3CN solution containing $Pb(OAc)_4$ (0.1 mM) and HBT (3 mM) at 25 °C in the absence (solid line) or in the presence (dashed line) of ferrocene (1 mM).

The reactions, however, were too fast to be followed spectrophotometrically and the kinetic studies were therefore carried out by laser flash photolysis, with the Z-BTNO radicals being produced by hydrogen atom abstraction from the corresponding *N*-hydroxy derivatives (Z-HBT) to the cumyloxyl radical generated by 355 nm laser flash photolysis of dicumyl peroxide (eqs 3−5 in Scheme 1).

The absorption spectra obtained after 355 nm laser excitation of a solution of dicumyl peroxide (0.8 M) and Z-HBT (1.9 mM)

---

(26) This value is ca. 0.1 V lower than that determined with pyridine instead of collidine as HBT deprotonating base.[8,20] However, it has to be noted that the same variation in the $E°$ value has been observed for the PINO/PINO$^-$ couple by changing the HPI deprotonating base (0.78 V[13] and 0.69 V[24] vs. SCE with pyridine and collidine, respectively).

(27) In the ring-substituted PINO anions no resonance structures can be described that delocalize the negative charge in the aromatic ring and only an inductive effect is exerted by the substituents.

(28) Galli, C.; Gentili, P.; Lanzalunga, O.; Lucarini, M.; Pedulli, G. F. *Chem. Commun.* **2004**, 2356–2357.

(29) 6-MeO-BTNO was not stable enough in the time scale of the spectrophotometric analysis, an increase of absorbance rapidly following its formation. Further studies are needed in order to understand the origin of the low stability of this *N*-oxyl radical.

(30) Frey, J. E.; Du Pont, L. E.; Puckett, J. J. *J. Org. Chem.* **1994**, *59*, 5386–5392.

SCHEME 1

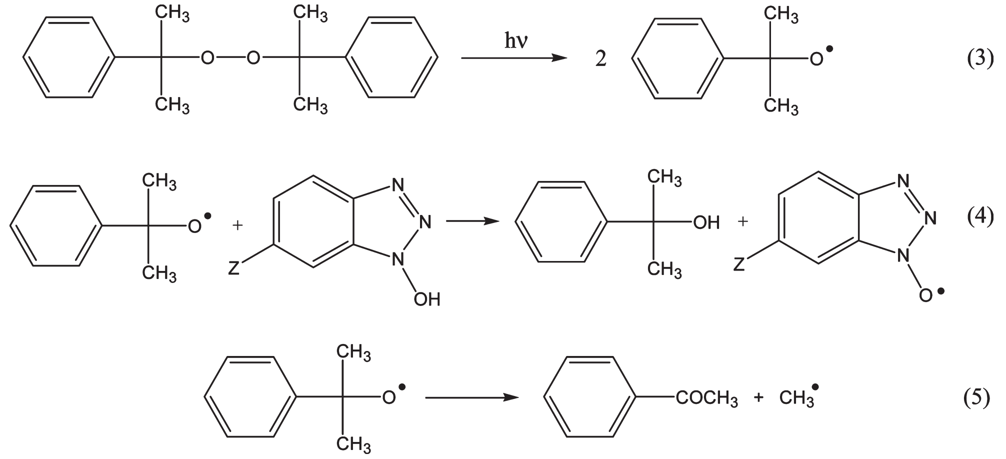

in N_2 saturated CH_3CN at 25 °C are similar to those recorded spectrophotometrically by oxidation of Z-HBT by $Pb(OAc)_4$ (see above). Values of the visible absorption maximum wavelengths are given in the third column of Table 1.

Due to the spectral overlap of the absorption bands of the cumyloxyl radical (λ_{max} = 490 nm)[31] and of the aminoxyl radicals (λ_{max} 450−485 nm), the rate of hydrogen abstraction from Z-HBTs (k_H) by the cumyloxyl radical was measured only for 6-CF_3-HBT, where it was possible to follow the simultaneous decay of the cumyloxyl radical and the buildup of the 6-CF_3-BTNO radical (see Figures S10 and S11 in the Supporting Information).

The second-order rate constant ($k_H = 2.2 \times 10^8$ M^{-1} s^{-1}) was significantly higher than that observed in the HAT from *N*-hydroxyphthalimide to the cumyloxyl radical ($k_H = 5.1 \times 10^7$ M^{-1} s^{-1}),[24] which suggests that the NO-H BDE in 6-CF_3-HBT (the highest in the HBT series under consideration[32]) is still lower than the NO-H BDE in HPI.

The rates of the ET reactions from substituted ferrocenes to the BTNO radical were measured by determining the decay rate of BTNO, generated as described above, in the presence of variable concentrations of ferrocene derivatives. The time-resolved spectra obtained after 355 nm LFP of an N_2-saturated CH_3CN solution containing dicumyl peroxide (0.8 M), HBT (8.3 mM), and ferrocene (0.1 mM) at T = 25 °C are displayed in Figure 5.

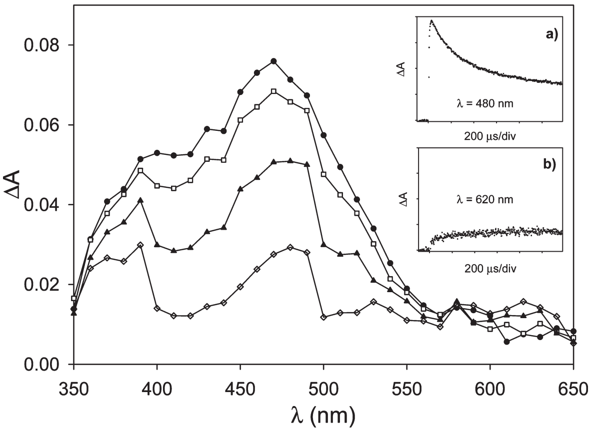

FIGURE 5. Time-resolved absorption spectra observed after 355 nm LFP of an N_2-saturated CH_3CN solution (T = 25 °C) containing dicumyl peroxide (0.8 M), HBT (8.3 mM), and ferrocene (0.1 mM), at 2.3 (circles), 8.0 (squares), 24 (triangles), and 115 µs (diamonds) after the 8 ns, 20 mJ laser flash. Inset a: Decay of the absorption of BTNO at 480 nm. Inset b: Buildup of the absorption of the ferricinium ion at 620 nm.

The absorption spectrum of the BTNO radical, recorded 2.3 µs after the laser pulse (filled circles), undergoes a first-order decay (inset a) accompanied by the formation of the ferrocenium ion (inset b), which displays the characteristic visible absorption band at λ_{max} = 620 nm.[30] An isosbestic point can be identified at λ = 580 nm.

In the presence of an excess of substituted ferrocenes FcX, a fast decay of the BTNO radical occurs that follows pseudo-first-order kinetics. When the observed rate constants (k_{obs}) for the decay measured at 480 nm were plotted against the concentration of FcX, excellent linear dependencies were observed (Figure 6), and the second-order rate constants (k_{et}) for the one-electron oxidation of FcX by BTNO were obtained from the slopes of these plots.

The kinetic data are collected in Table 2, together with the redox potentials of the ferrocenes measured by cyclic voltammetry[24] and the ET free energies $\Delta G°_{et}$. For the calculation of the latter values we used the $E°$ value for the BTNO/$BTNO^-$ couple (0.63 V vs. SCE) measured by cyclic voltammetry in CH_3CN (see the Experimental Section). For comparison, in Table 2 are also reported the rate constants for the corresponding reactions of FcX with PINO.[24]

Likewise, the kinetic analysis of the ET reactions from ferrocene (FcH) to ring-substituted benzotriazole-*N*-oxyl radicals (Z-BTNO, Z = H, 6-CF_3, 6-Cl, 6-Me, 6-MeO) was carried out by following the decay of the Z-BTNO radicals at the maximum absorption wavelength (see Table 1) as a function of the FcH concentration. In this case too, when the pseudo-first-order rate constants (k_{obs}) for the decay of Z-BTNOs were plotted against the concentration of FcH, excellent linear dependencies were observed (see Figure S13 in the Supporting Information), and the second-order rate constants (k_{et}) for the one-electron oxidation of FcH by

---

(31) Avila, D. V.; Lusztyk, J.; Ingold, K. U. *J. Am. Chem. Soc.* **1992**, *114*, 6576–6577. Avila, D. V.; Ingold, K. U.; Di Nardo, A. A.; Zerbetto, F.; Zgierki, M. Z.; Lusztyk, J. *J. Am. Chem. Soc.* **1995**, *117*, 2711–2718.

(32) The NO-H BDE for 6-CF_3-HBT is unknown. However, electron-withdrawing substituents are expected to increase the NO-H BDE value as found in the series of aryl-substituted HPIs.[18]

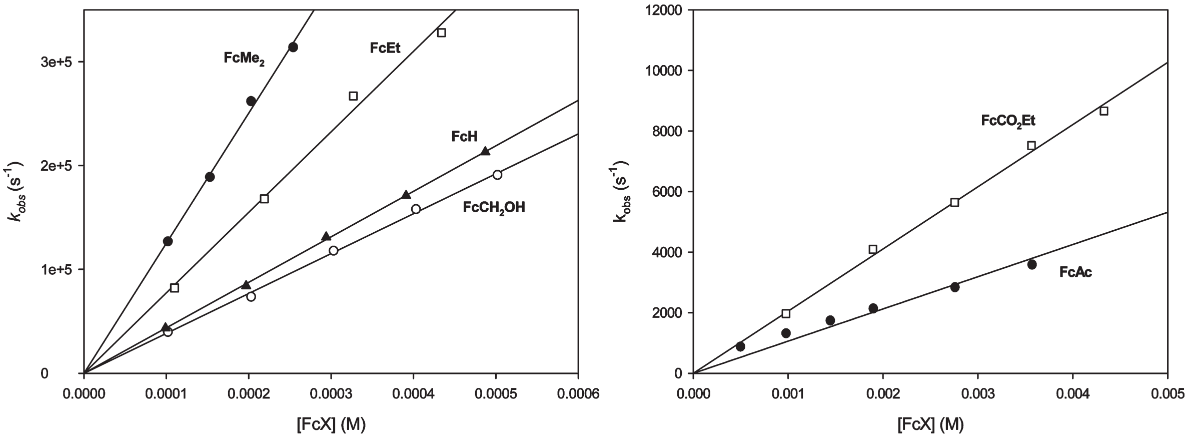

FIGURE 6. Dependence of the observed rate constants (k_{obs}) for the decay of BTNO on the concentrations of ferrocenes FcX in CH_3CN at 25 °C. The slope of the plots gives the k_{et} values.

TABLE 2. Oxidation Potentials of Ferrocenes (FcX) in CH_3CN ($E°$), Electron-Transfer Free Energies ($\Delta G°_{et}$), and Second-Order Rate Constants (k_{et}) for the Reaction of FcX with BTNO in CH_3CN at 25 °C,[a] and Second-Order Rate Constants for the Reaction of FcX with PINO[b]

			k_{et} ($M^{-1}s^{-1}$)[d]	
FcX	$E°$ (V vs. SCE)[b]	$\Delta G°_{et}$ (kcal mol^{-1})[c]	BTNO	PINO[b]
FcH	0.41	−5.1	$4.4 \pm 0.1 \times 10^8$	$1.5 \pm 0.1 \times 10^7$
FcMe$_2$	0.29	−7.8	$1.3 \pm 0.1 \times 10^9$	$1.8 \pm 0.1 \times 10^8$
FcEt	0.34	−6.7	$7.6 \pm 0.2 \times 10^8$	$7.2 \pm 0.3 \times 10^7$
FcCH$_2$OH	0.40	−5.3	$3.8 \pm 0.1 \times 10^8$	$4.3 \pm 0.3 \times 10^7$
FcCO$_2$Et	0.65	0.5	$2.1 \pm 0.1 \times 10^6$	$< 10^5$
FcAc	0.66[e]	0.7	$8.4 \pm 0.3 \times 10^5$	n.d.

[a] Dicumyl peroxide (0.8 M), HBT (8.3 mM), ferrocenes (0.1−4.3 mM). [b] Reference 24. [c] Determined on the basis of an $E°_{red}$ value of 0.63 V vs. SCE for BTNO (see text). [d] Determined by LFP from the slopes of the k_{obs} for the decay of the N-oxyl radicals vs. the FcX concentration. [e] Reference 33.

TABLE 3. Electron-Transfer Free Energies ($\Delta G°_{et}$) and Second-Order Rate Constants (k_{et}) for the Reaction of Ferrocene with Z-BTNOs in CH_3CN at 25 °C[a]

N-oxyl radical	$\Delta G°_{et}$[b]	k_{et} (M^{-1} s^{-1})[c]
6-CF$_3$−BTNO	−8.1	$1.5 \pm 0.1 \times 10^9$
6-Cl-BTNO	−6.7	$1.4 \pm 0.1 \times 10^9$
BTNO	−5.1	$4.4 \pm 0.1 \times 10^8$
6-Me-BTNO	−4.4	$2.4 \pm 0.1 \times 10^8$
6-MeO-BTNO	−3.9	$1.8 \pm 0.1 \times 10^8$

[a] Dicumyl peroxide (0.8 M), Z-HBT (3.3−8.2 mM), ferrocene (0.05−0.6 mM). [b] In kcal mol^{-1}, on the basis of an $E°_{red}$ value of 0.41 V vs. SCE for ferrocene. [c] Determined from the slopes of the k_{obs} for the decay of the Z-BTNO radicals vs. ferrocene concentration.

Z-BTNOs were obtained from the slopes of these plots. All the kinetic data are collected in Table 3, where the ET free energies $\Delta G°_{et}$ are also displayed.

Discussion

The data in Table 2 show that the second-order rate constants for the electron transfer from substituted ferrocenes to the BTNO radical (k_{et}) are very sensitive to the oxidation potential of the substrate increasing by decreasing the $E°$ value, i.e., as the free energy change of the ET step ($\Delta G°_{et}$) decreases. A first important notation is that, where the comparison is possible, the k_{et} values for BTNO are significantly higher than those observed in the corresponding reactions with PINO.[24] The pertinent data are in Table 2, where we can see that the reactivity of BTNO is at least an order of magnitude higher than that of PINO. The maximum difference (30 times) is observed with ferrocene. As a consequence, with BTNO it was also possible to measure the rates of the one-electron oxidation of the less oxidizable ferrocenes (FcAc and FcCO$_2$Et) that could not be measured in the corresponding reactions with the PINO radical. If we consider that the redox potential of the BTNO radical is ca. 60 mV lower than that of the PINO radical (see Table 1), the above observations indicate that the intrinsic reactivity of BTNO in one-electron oxidation is significantly higher than that of PINO.

This difference can be put on a quantitative basis by plotting the ln k_{et} values against the free energy change of the ET step corrected for the electrostatic contribution arising from the charge variation in the reactants upon electron transfer ($\Delta G°'$)[34] according to eq 6, which combines the Marcus and Eyring equations.[37,38] In eq 6 λ is the reorgani-

---

(33) Determined by cyclic voltammetry under the same experimental conditions used for the other ferrocenes (see the Experimental Section and Figure S12 in the Supporting Information).

(34) $\Delta G°'$ values are calculated from the $\Delta G°_{et}$ values reported in Tables 2 and 3 according to the following equation: $\Delta G°' = \Delta G°_{et} + (Z_1 - Z_2 - 1)(e^2 f / D r_{12})$, where e is the electron charge, Z_1 and Z_2 are the charge numbers of the reactants, r_{12} is the distance between BTNO and the ferrocenes in the encounter complex (taken as 7.2 Å),[35] D is the dielectric constant of the solvent (35 for CH_3CN), and f is a factor depending upon the ionic strength ($f \cong 1$ for $\mu \rightarrow 0$). The values of $\Delta G°'$ are listed in Table S1 (ET reactions from ferrocenes (FcX) to BTNO) and Table S2 (ET reactions from ferrocene to Z-BTNO) in the Supporting Information.

(35) The radius of ferrocene is 2.6 Å.[36] The radius of BTNO (4.6 Å) was calculated from the volume of BTNO (404 Å^3) given by the Hyperchem program.

(36) Carlson, B. W.; Miller, L. L.; Neta, P.; Grodkowski, J. *J. Am. Chem. Soc.* **1984**, *103*, 7233–7239.

(37) Marcus, R. A. *Annu. Rev. Phys. Chem.* **1964**, *15*, 155–196.

(38) Eberson, L. *Electron Transfer Reactions in Organic Chemistry*; Springler Verlag: Berlin , Germany, 1986; Chapter 3.

zation energy and Z is the bimolecular collision frequency. The satisfactory fit of the experimental data to eq 6 is shown in Figure 7 ($r^2 = 0.947$, see the Supporting Information for the calculation details).

$$k_{\mathrm{et}} = Z\mathrm{e}^{-(\lambda + \Delta G^{\circ\prime})^2/4\lambda RT} \qquad (6)$$

From the nonlinear least-squares fitting, a λ value of 31.1 kcal mol^{-1} can be calculated for the reorganization energy required in the transfer of one electron from ferrocene derivatives to BTNO. Assuming that the value of the ET self-exchange reorganization energy for the ferrocene/ferrocenium couple ($\lambda_{\mathrm{Fc^+/Fc}}$) is 27.5 kcal mol^{-1} in MeCN,[24,39] the reorganization energy for the BTNO/BTNO$^-$ couple ($\lambda_{\mathrm{BTNO/BTNO^-}}$) can be calculated from eq 7 as 34.7 kcal mol^{-1}.

$$1/2(\lambda_{\mathrm{BTNO/BTNO^-}} + \lambda_{\mathrm{Fc^+/Fc}}) = 31.1 \qquad (7)$$

This value is more than 14 kcal mol^{-1} lower than that determined previously for the PINO/PINO$^-$ couple (49.1 kcal mol^{-1}).[24] Clearly, this significant difference in the kinetic barrier appears sufficient to overcome the thermodynamic factor, which is slightly in favor of PINO, so making BTNO a better one-electron oxidant than PINO.

In line with this conclusion are the results of the study of the one-electron oxidation of ferrocene by ring-substituted benzotriazole-*N*-oxyl radicals (Z-BTNO, Z=H, 6-CF$_3$, 6-Cl, 6-Me, 6-MeO). The second-order rate constants (k_{et}), reported in Table 3, increase by increasing the electron-withdrawing power of the Z substituent, i.e., by decreasing the free energy change of the ET process ($\Delta G^{\circ}_{\mathrm{et}}$), and in accordance a satisfactory fit with the Hammett equation with a positive ρ value (1.24) was obtained by plotting the log ($k_{\mathrm{et}}^{\mathrm{Z}}/k_{\mathrm{et}}^{\mathrm{H}}$) values against the σ_{p} constants (Figure S14 in the Supporting Information).

When the ln k_{et} values were plotted against the $\Delta G^{\circ\prime}$ values, according to eq 6, again a satisfactory fit was obtained (Figure 8, $r^2 = 0.919$) and it was very rewarding to observe that the reorganization energy value (λ) required for the electron-transfer process from ferrocene to Z-BTNOs calculated from the nonlinear least-squares fitting (29 kcal mol^{-1}) is quite close to that determined in the reaction between substituted ferrocenes and the BTNO radical discussed above. By applying eq 7, a value of ca. 30.5 kcal mol^{-1} can be calculated for the ET self-exchange reorganization energy of the BTNO/BTNO$^-$ couple ($\lambda_{\mathrm{BTNO/BTNO^-}}$), which again compares reasonably well with that (34.7 kcal mol^{-1}) obtained above from the reaction of BTNO with substituted ferrocenes. It can be added that the fit in Figure 8 suggests that the self-exchange reorganization energy for the BTNO/BTNO$^-$ couple is not significantly influenced by the presence of substituents on the aryl ring.

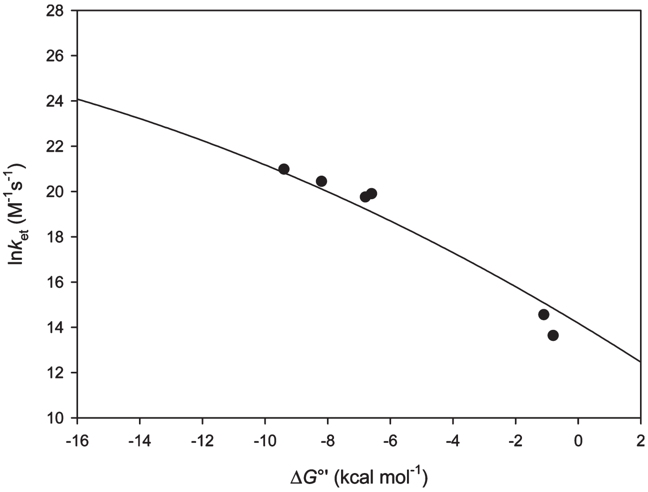

FIGURE 7. Diagram of ln k_{et} vs. $\Delta G^{\circ\prime}$ for the reactions of substituted ferrocenes with BTNO. The solid circles correspond to the experimental values; the curve is calculated by nonlinear least-squares fit to eq 6.

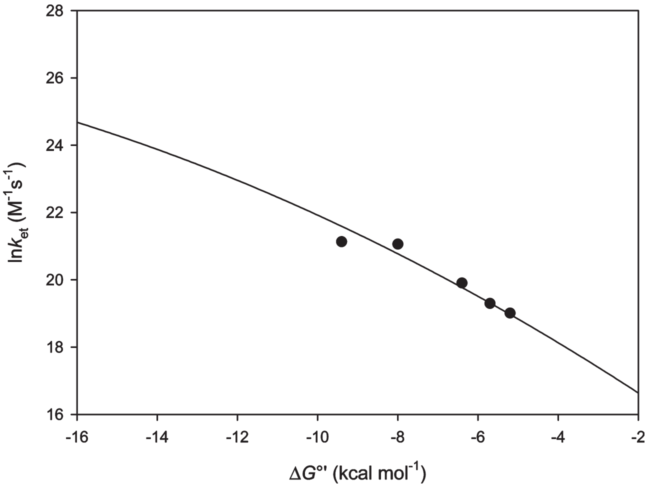

FIGURE 8. Diagram of ln k_{et} vs. $\Delta G^{\circ\prime}$ for the reactions of ferrocene with Z-BTNO. The solid circles correspond to the experimental values; the curve is calculated by nonlinear least-squares fit to eq 6.

If we take 32.3 kcal mol^{-1} as the value of $\lambda_{\mathrm{BTNO/BTNO^-}}$ (the average of the two values calculated above) we can calculate a rate of the self-exchange reaction for the BTNO/BTNO$^-$ couple of 7.6×10^5 M^{-1} s^{-1}, a value that is 3 orders of magnitude higher than that calculated for the PINO/PINO$^-$ couple (760 M^{-1} s^{-1}).[24]

Thus, there should be no doubt that the intrinsic reactivity of BTNO in one-electron oxidations is significantly higher than that of PINO and it is very difficult to find a simple explanation for a so remarkable difference. An observation that might be useful in this respect is that the two *N*-oxyl radicals and the corresponding anions exhibit quite relevant differences with respect to the extent of spin density (the radicals) and negative charge delocalization (the anions) in the benzene ring. Namely, the spin delocalization is larger in the BTNO than in PINO and the charge delocalization is larger in BTNO$^-$ than in PINO$^-$. Accordingly, in BTNO the hyperfine coupling constants with three unequivalent

---

(39) The ferrocenes investigated should have very close self-exchange reorganization energies and in agreement similar self-exchange rate values have been reported by Wahl et al. for ferrocene, 1,1′-dimethylferrocene, di-*n*-butylferrocene, and methyl ferrocenecarboxylate.[40] Small differences in the self-exchange reorganization energies have also been reported for ferrocene, chloromercuryferrocene, butylferrocene, and 1,1′-dimethylferrocene.[41] Thus, the ET self-exchange reorganization energy for the ferrocene/ferrocenium couple ($\lambda_{\mathrm{Fc^+/Fc}}$) should hold, at least to a first approximation, also for the substituted ferrocenes.

(40) Yang, E. S.; Chan, M.-S.; Wahl, A. C. *J. Phys. Chem.* **1980**, *84*, 3094–3099.

(41) Pladziewicz, J. R.; Espenson, J. H. *J. Am. Chem. Soc.* **1973**, *95*, 56. Eberson, L.; Barry, J. E.; Finkelstein, M.; Moore, W. M.; Ross, S. D. *Acta Chem. Scand.* **1986**, *B40*, 283–294.

TABLE 4. Comparison of Second-Order Rate Constant (k_H) for H-Abstraction from Several H-Donor Substrates to PINO and BTNO Radicals at 25 °C in CH_3CN

	k_H (M^{-1} s^{-1})	
substrate, RH	BTNO[a]	PINO
$C_6H_5CH_2OH$	0.94	15.6[b]
cyclohexanol	0.33	4.52[b]
C_6H_5OH	66	330[c]
fluorene	1.9	26.2[b]
$(C_6H_5)_2CHOH$	3.2	33.2[b]

[a] Normalized for the number of equivalent H-atoms in RH. Reference 20. [b] PINO generated electrochemically in CH_3CN from ref 13. [c] From ref 22.

protons are 0.037, 0.203, and 0.458 mT[28] whereas in PINO the hyperfine coupling constant with the ring protons is only 0.045 mT.[21] Concerning the larger charge delocalization in $BTNO^-$ than in $PINO^-$, this is indicated by the previously noted larger sensitivity to the electronic effects of the aryl substituents on the $E°$ values for the BTNO/$BTNO^-$ couple than for the PINO/$PINO^-$ couple (see above). Thus, it seems not unreasonable to suggest that the larger spin and charge delocalization in the BTNO/$BTNO^-$ couple may play a role in decreasing the intrinsic barrier for the self-exchange electron-transfer process with respect to that in the PINO/$PINO^-$ system. It should also be noted that spin and charge delocalization might also exert their effect by influencing the energy associated to the solvent reorganization, which might be a very important factor in the determination of the intrinsic barrier.[42] Of course, this is at most a working hypothesis and certainly a full comprehension of the remarkable difference in the electron-transfer intrinsic barriers between BTNO and PINO will require thorough theoretical calculations which should also be concerned with the role of the solvent.

Finally, a noteworthy observation is that the higher reactivity of BTNO with respect to PINO in the ET reaction with ferrocene sharply contrasts with the situation observed in HAT processes where, as already mentioned, PINO is the most reactive species,[19,20] as clearly shown by some literature data collected in Table 4.

Clearly, in HAT processes the reactivity appears dominated by the thermodynamic factor as the O−H bond formed by PINO is ca. 3 kcal mol^{-1} stronger than that formed by BTNO.[8,19,20] From this contrast, an interesting hypothesis is that in the oxidation reactions promoted by these short-lived *N*-oxyl radicals, the PINO/BTNO relative reactivity might represent a criterion to help to distinguish between ET and HAT mechanisms. A reactivity with BTNO larger than with PINO would suggest a ET mechanism. On the contrary, a HAT mechanism would be deemed more probable when PINO is more reactive than BTNO. Work is in progress to find further examples which may confirm this conclusion.

Experimental Section

Starting Materials. CH_3CN (spectrophotometric grade) was distilled over CaH_2. Commercial samples of dicumyl peroxide, 1-hydroxybenzotriazole, 6-chloro-1-hydroxybenzotriazole (6-Cl-HBT), and 6-trifluoromethyl-1-hydroxybenzotriazole (6-CF_3-HBT) were used as received. 6-Methyl-1-hydroxybenzotriazole (6-Me-HBT) and 6-methoxy-1-hydroxybenzotriazole (6-MeO-HBT) were synthesized as described in the literature.[43,44] Ferrocene (FcH), acetylferrocene (FcAc), ferrocenemethanol (Fc-CH_2OH), ethylferrocene (FcEt), and 1,1′-dimethylferrocene ($FcMe_2$) are commercially available and were further purified by sublimation or by column chromatography on silica gel with toluene as eluent (FcEt). Ethyl ferrocenecarboxylate ($FcCO_2Et$) was prepared by esterification of commercially available ferrocenecarboxylic acid with ethanol according to the literature.[45]

Cyclic Voltammetry. Cyclic voltammetry at the steady disk electrode (glassy carbon disk, 1.5 mm in diameter) was carried out at 25 °C in CH_3CN containing the Z-HBT (2.0 mM) or FcAc (2.0 mM) and Bu_4NBF_4 (0.1 M) as supporting electrolyte. In the experiment with Z-HBT, in order to generate Z-$BTNO^-$, collidine (4 mM) was added to the CH_3CN solution. A three-electrode circuit was used with a homemade potentiostat with positive feedback ohmic drop compensation and PLI hardware (Vernier Software & Technology) controlled by a program written in C++ language for Windows 95/98. The auxiliary electrode was a platinum wire (surface 1 cm^2), and an Ag/AgCl (KCl, 3 M) electrode was used as reference; the redox potential values are then referred to SCE. The sweep scan was 500 mV/s.

Spectrophotometric Studies. Z-BTNOs were generated in a 3 mL quartz cuvette (10 mm × 10 mm) by the oxidation of Z-HBT (3 mM) with $Pb(OAc)_4$ (0.1 mM) in CH_3CN at 25 °C and under an argon atmosphere and their UV−vis absorption spectra were recorded. When a solution of substituted ferrocenes FcX was then added into the BTNO solution in a 1 cm quartz cuvette (substrate concentration 1 mM), the absorption of BTNO disappeared and was replaced by that of the ferrocenium cations. In the same way the absorption of Z-BTNO was replaced by that of ferrocenium when a solution of ferrocene was added to the Z-BTNO solutions in the cuvette.

Laser Flash Photolysis Experiments. Laser flash photolysis experiments were carried out with an Applied Photophysics LK-60 laser kinetic spectrometer providing 8 ns pulses, using the third armonic (355 nm) of a Quantel Brilliant-B Q-switched Nd:YAG laser. The laser energy was adjusted to ≤10 mJ/pulse by the use of the appropriate filter. A 3 mL Suprasil quartz cell (10 mm × 10 mm) was used for all the experiments. N_2-saturated CH_3CN solutions of dicumyl peroxide (0.8 M), ring-substituted-1-hydroxybenzotriazoles (3.3−8.2 mM), and ferrocenes (0.05−4.3 mM) were used. All the experiments were carried out at $T = 25 \pm 0.5$ °C under magnetic stirring. Data were collected at individual wavelengths with an Agilent Infinium oscilloscope and analyzed with the kinetic package implemented in the instrument. Rate constants were obtained by monitoring the change of absorbance at the maximum absorption wavelength and by averaging 3−5 values. Each kinetic trace obeyed a first-order kinetic and second-order rate constants were obtained from the slopes of the plots of the observed rate constants k_{obs} vs. substrate concentration.

Acknowledgment. Financial support from the Ministero dell'Istruzione dell'Università e della Ricerca (MIUR) is gratefully acknowledged. We thank Prof. Lorenzo Stella for the use and assistance in the use of LFP equipment and Dr. Patrizia Gentili for technical assistance in the cyclic voltammetry.

---

(42) Some very simple preliminary calculations carried out for the PINO/$PINO^-$ couple suggested that most of the reorganization energy may involve the reorganization of the solvent.[23]

(43) Munson, J. W.; Hodgkins, T. G. *J. Heterocycl. Chem.* **1978**, *15*, 545–550.

(44) Konig, W.; Geiger, R. *Chem. Ber.* **1970**, *103*, 788–798.

(45) Top, S.; Masi, S.; Jaouen, G. *Eur. J. Inorg. Chem.* **2002**, 1848–1853.

Supporting Information Available: UV−vis absorption spectra for the reactions of BTNO with FcX and of Z-BTNOs with FcH (spectrophotometric studies), transient absorption spectra and dependence of k_{obs} on [6-CF_3-HBT] for the HAT from 6-CF_3-HBT to the cumyloxyl radical in CH_3CN, dependence of k_{obs} for the decay of Z-BTNOs on the concentration of FcH, Hammett plot for the reactions of ferrocene with Z-BTNO, cyclic voltammetry of FcAc and Z-BTNO/Z-BTNO$^-$ in MeCN, and determination of the reorganization energy. This material is available free of charge via the Internet at http://pubs.acs.org.